

Life in Crowded and Disordered Environments

Andrea Giansanti

Dipartimento di Fisica, Sapienza Università di Roma

Andrea.Giansanti@roma1.infn.it

From chapter 14, Physical Biology of the Cell
LECTURE 19 may 9 2018

DIPARTIMENTO DI FISICA



SAPIENZA
UNIVERSITÀ DI ROMA

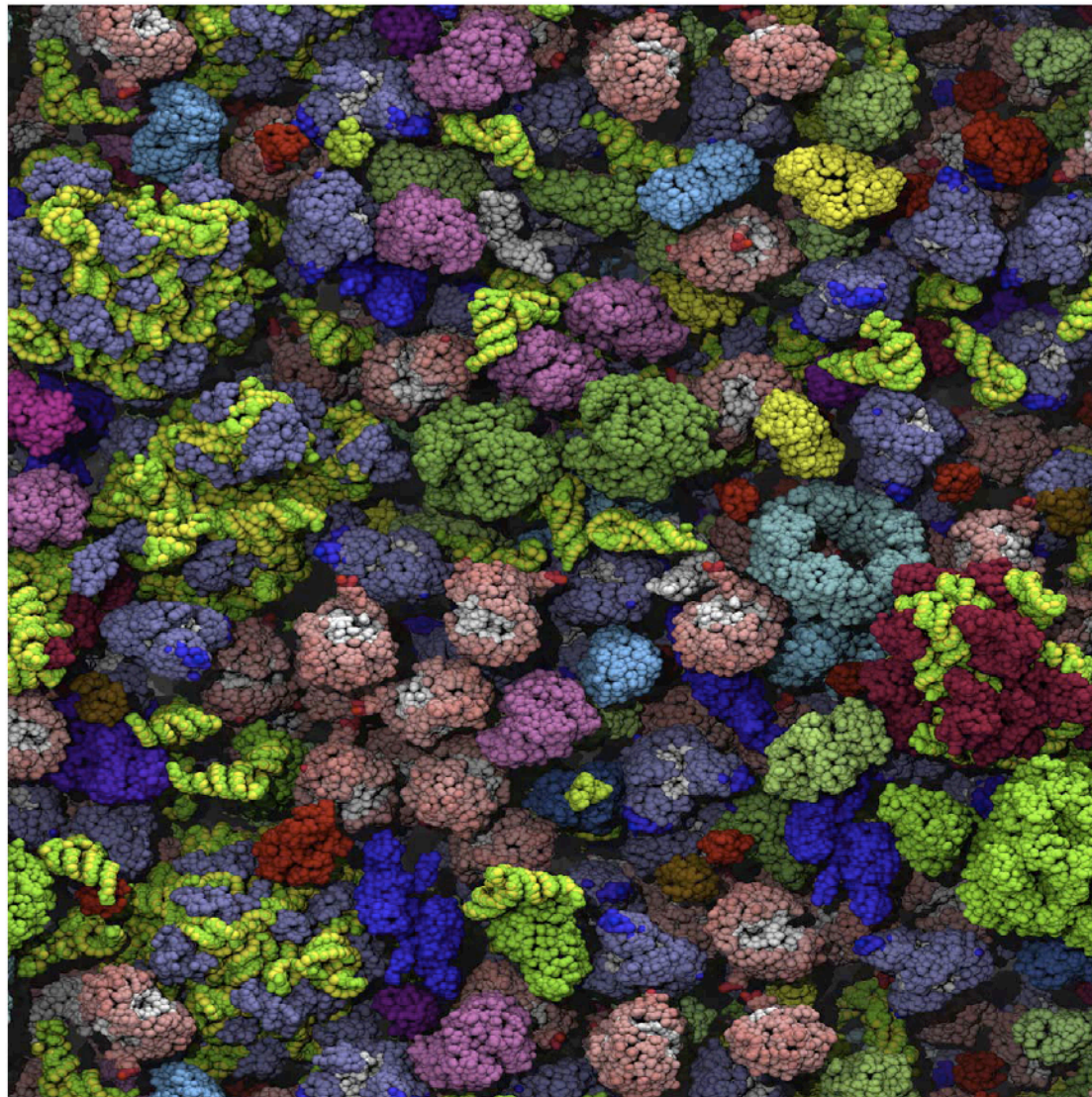
INTRODUCTORY REMARKS

How to correct the treatment of binding and of diffusion
in a crowded environment

Where ideality (dilution) and homogeneity are quite untenable

Nevertheless consider the effectiveness of the free electron model
of metal conductivity...a reductionist approach is not out of scope

See: JT Mika and B Poolman, *Macromolecule diffusion and confinement in prokaryotic cells*
Current Opinion in Biotechnology 2011, 22:117–126



Current Opinion in Biotechnology

Crowding in the cytoplasm of bacteria. A snapshot of the *E. coli* cytoplasm at a macromolecule concentration (275 g/L) approximating *in vivo* conditions [2*]. With permission from Adrian Elcock.

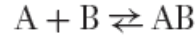
Just an estimate of relative crowding, e.g. the *E. coli* membrane

Just as simple estimates on protein concentrations in the cytoplasm reveal a mean spacing comparable to protein size, similar estimates can be carried out for the cell membrane as well. To see this, we recall that the membrane area for a bacterium like *E. coli* is roughly $6\mu\text{m}^2$ and that both the inner and outer membranes are home to roughly 500,000 proteins. This tells us that the area per protein is roughly 10nm^2 , or that the typical distance between two proteins is of the order of 3 nm. The cell membrane is tightly packed indeed.

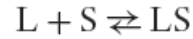
Crowding alters chemical equilibria: additional free energy terms lead to altered reaction constants w.r. to the free case

Three kind of equilibrium reactions displaced by crowding (from Zhou et al. 2008 annu. rev. biophys.)

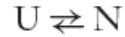
Bimolecular Association



Association of a Soluble Macromolecular Ligand with a Specific Surface Binding Site



Two-State Folding of a Protein



$$\Delta F_{AB} = -RT \ln K_{AB},$$

$$\Delta F_{LS} = -RT \ln K_{LS},$$

$$\Delta F_{UN} = -RT \ln K_{UN},$$

$$\begin{aligned} \Delta\Delta F_{AB} &\equiv \Delta F_{AB} - \Delta F_{AB}^0 \\ &= \Delta F_{AB}^C - \Delta F_A^C - \Delta F_B^C, \quad 1. \end{aligned}$$

$$\Delta\Delta F_{LS} \equiv \Delta F_{LS} - \Delta F_{LS}^0 = \Delta F_{LS}^C - \Delta F_L^C, \quad 2.$$

$$\begin{aligned} \Delta\Delta F_{UN} &\equiv \Delta F_{UN} - \Delta F_{UN}^0 \\ &= \Delta F_N^C - \Delta F_U^C, \quad 3. \end{aligned}$$

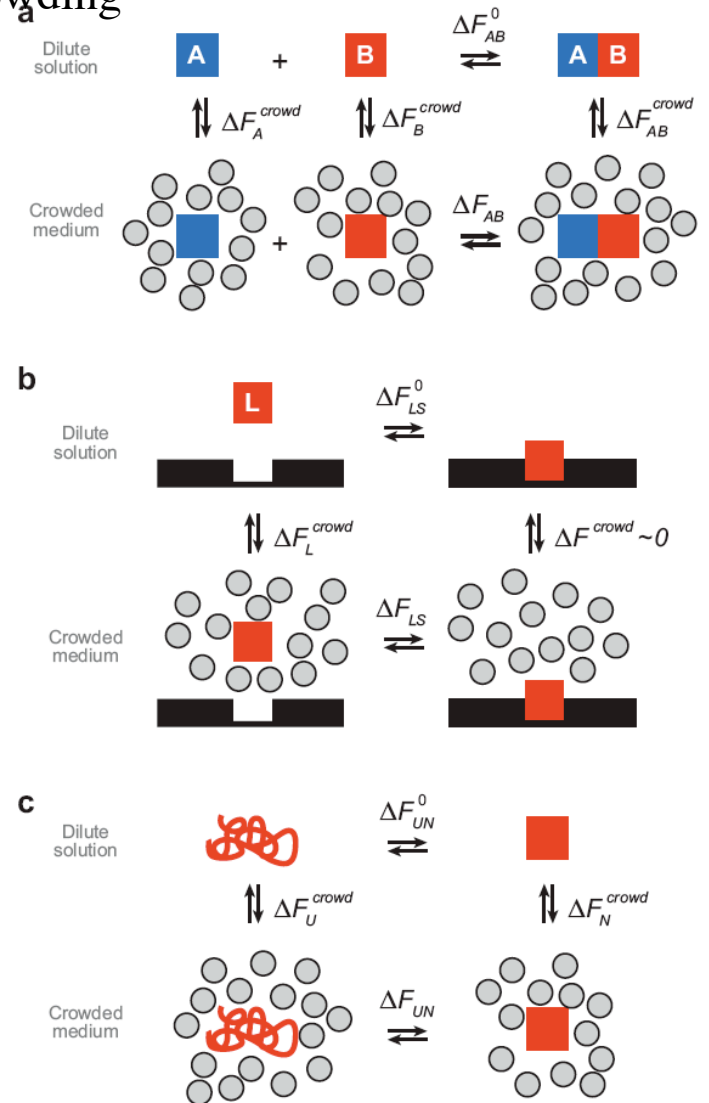


Figure 1

Thermodynamic cycles illustrating linkage between free energy of transfer of reactants and products from dilute solution to crowded medium and standard free energy of (a) association in solution, (b) site-binding, and (c) two-state folding of a protein.

Further remarks

¹Equations 1–3 apply equally to changes in Helmholtz or Gibbs free energies. Simple models used to estimate the magnitude of ΔF_X^C generally assume constant volume and hence in the strict sense yield estimates of Helmholtz free energy changes. However, differences between Helmholtz and Gibbs free energy changes associated with reactions in the liquid state are not of qualitative significance.

² ΔF_X^C is formally equivalent to the difference between the equilibrium average free energy of interaction of X with the perturbing cosolutes or boundaries and the equilibrium average free energy of interaction of X with the constituents of bulk solvent that are replaced by cosolute or boundary. Thus ΔF_X^C implicitly takes into account any energetic consequence of desolvation that may accompany the transfer.

³The treatment presented here may be readily extended to a quasi-equilibrium analysis of the effect of crowding or confinement upon the kinetics of a transition-state limited association or isomerization reaction, in which case one must additionally estimate the free energy change associated with the transfer of the transition state from bulk to the crowded or confined medium (see for example the Appendix in Reference 59).

Life is made by filamentous structures

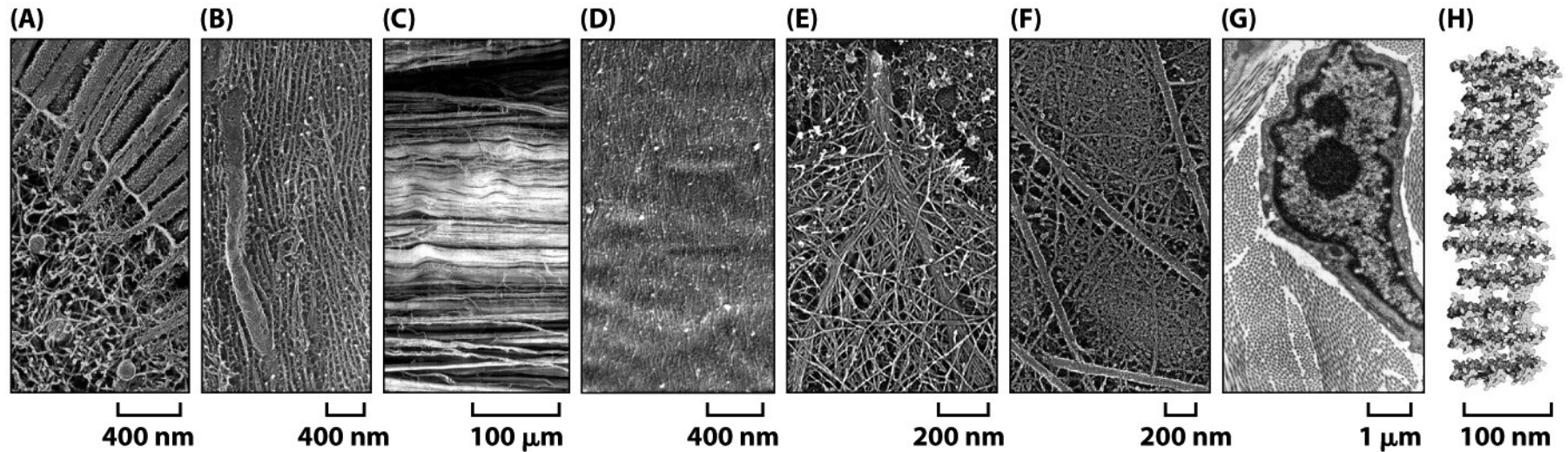
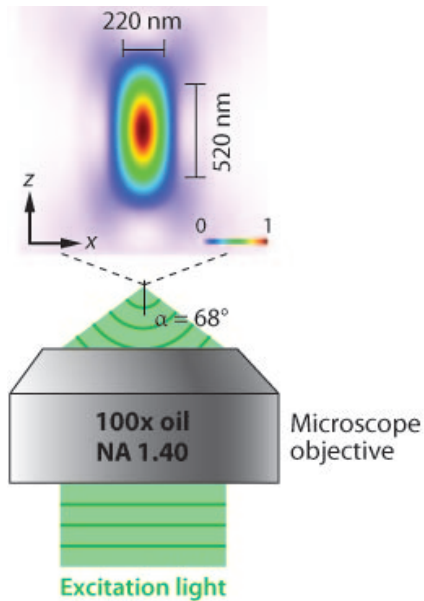


Figure 14.1 Physical Biology of the Cell (© Garland Science 2009)

See chap. 10



Huang B, et al. 2009.

Annu. Rev. Biochem. 78:993–1016

The Diffraction Limit

An optical microscope can be thought of as a lens system that produces a magnified image of a small object. In this imaging process, light rays from each point on the object converge to a single point at the image plane. However, the diffraction of light prevents exact convergence of the rays, causing a sharp point on the object to blur into a finite-sized spot in the image. The three-dimensional (3D) intensity distribution of the image of a point object is called the point spread function (PSF). The size of the PSF determines the resolution of the microscope: Two points closer than the full width at half-maximum (FWHM) of the PSF will be difficult to resolve because their images overlap substantially. The FWHM of the PSF in the lateral directions (the x-y directions perpendicular to the optical axis) can be approximated as $\Delta_{xy} \approx 0.61\lambda/\text{NA}$, where λ is the wavelength of the light, and NA is the numerical aperture of the objective defined as $\text{NA} = n \sin\alpha$, with n being the refractive index of the medium and α being the half-cone angle of the focused light produced by the objective. The axial width of the PSF is about 2–3 times as large as the lateral width for ordinary high NA objectives. When imaging with visible light ($\lambda \approx 550 \text{ nm}$), the commonly used oil immersion objective with $\text{NA} = 1.40$ yields a PSF with a lateral size of 200 nm and an axial size of 500 nm in a refractive index-matched medium

Annual Reviews

Actin networks and ergodicity breaking

Non homogeneity is dynamically sustained

Cells not only allow filament bundling and superstructural organization to happen but encourage it with cross-linking proteins that tie filaments together. Spontaneous alignment alone will give a mixed orientation of polar filaments, but in many of the examples seen in cells the filaments are all pointing in the same direction. This cannot arise from entropy alone, but rather emerges from local nucleating of sites to make sure everything grows in the same direction or from the exploitation of motor proteins to sort out filaments based on their orientations. This will be further discussed in Chapter 16. A higher resolution image of filamentous organization at the leading edge of a motile cell is shown in Figure 14.2. One of the intriguing features of this organization is that it varies as a function of distance from the leading edge itself. In

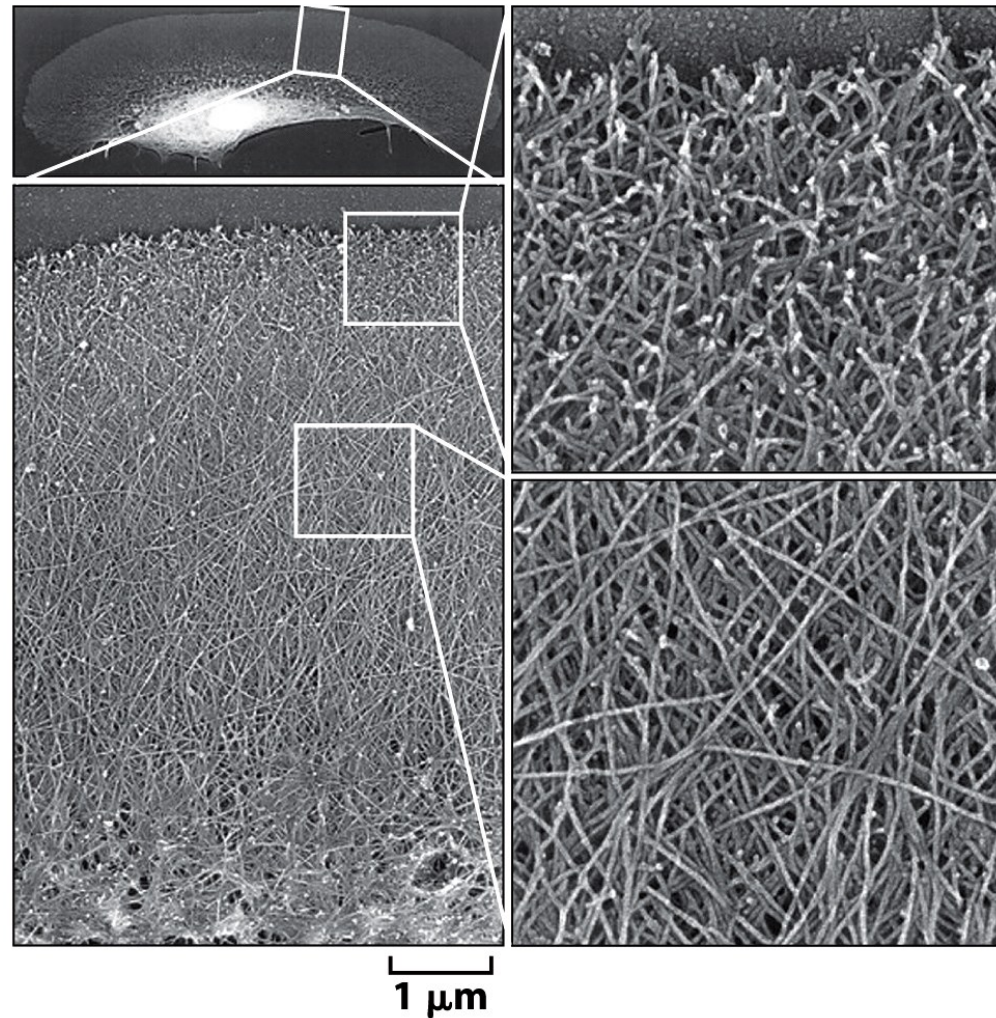


Figure 14.2 Physical Biology of the Cell (© Garland Science 2009)

videomicroscopy

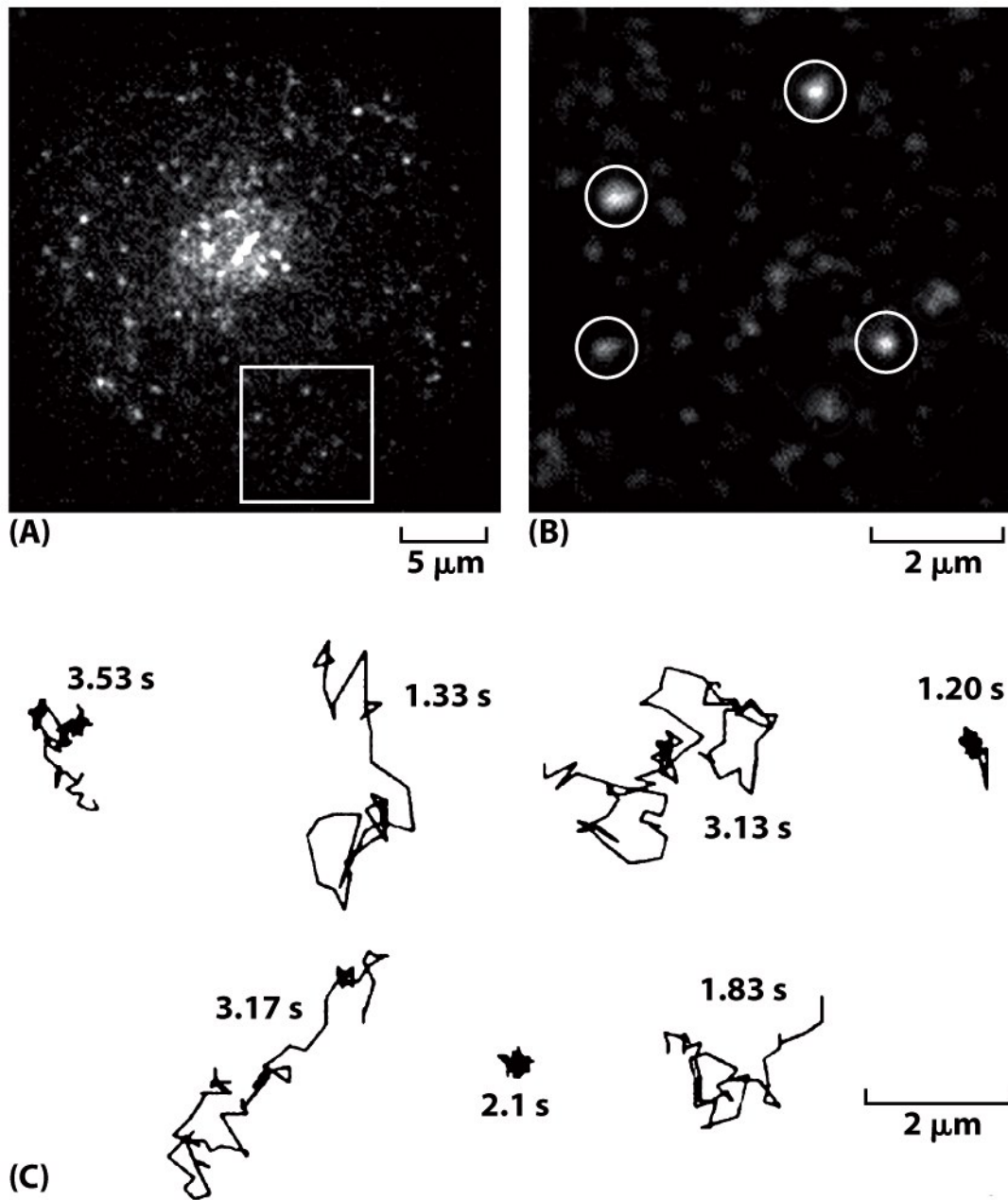


Figure 14.5 Single-molecule measurements for diffusion of membrane-associated proteins. (A) Cells were transfected with a construct encoding GFP fused to a membrane protein Lck. In the fluorescence microscope, the cells appear to be covered with randomly distributed spots. (B) In a magnified view of the region bounded by the box in (A), individual molecules can be clearly seen (circles). Their movements can be tracked over time by video microscopy. (C) A series of tracks measured for individual molecules ranging over total times of about 1–3.5 s show very heterogeneous individual behavior. Some molecules appear to be trapped and nearly stationary, while others travel long distances. (Adapted from A. D. Douglass and R. Vale, *Cell* 121:937, 2005.)

Cage effects:
Inhomogeneity of space

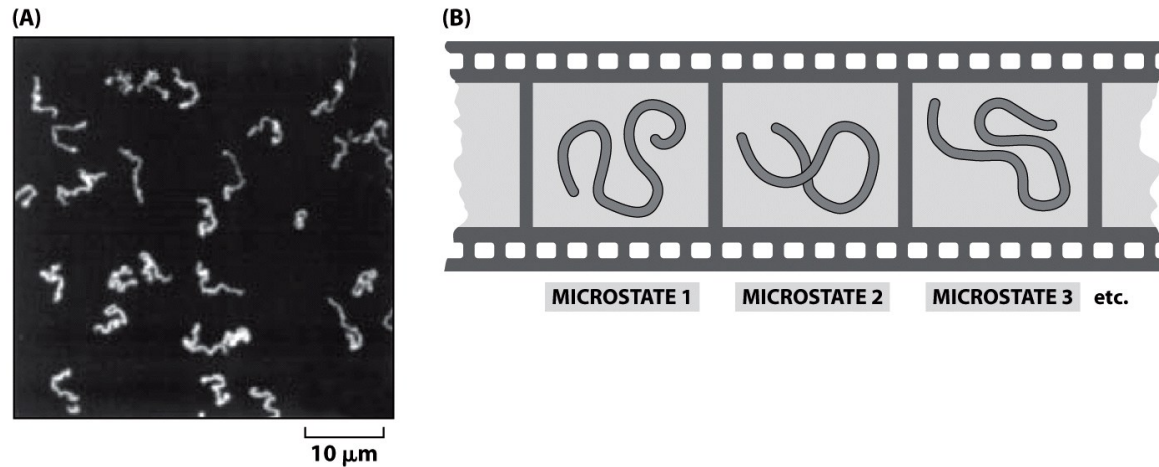


Figure 6.2 Physical Biology of the Cell (© Garland Science 2009)

Statistics out of dynamics:
Ergodicity concepts

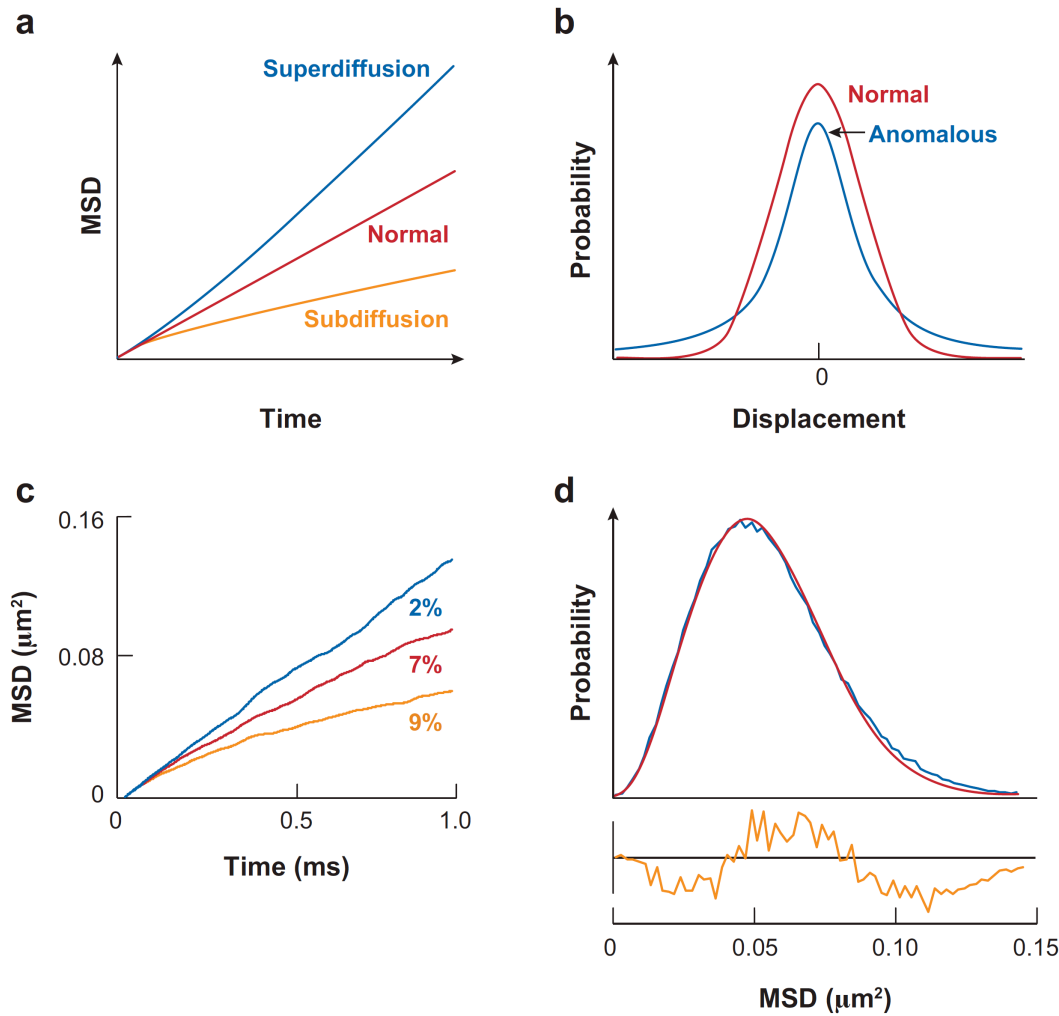


Figure 1

Characteristics and simulations of anomalous diffusion. (a) MSD curves defining normal (Brownian) diffusion and anomalous subdiffusion (downward curvature) and superdiffusion (upward curvature). (b) Distribution of displacements for normal and anomalous diffusion. Initial particle position is at the origin. For normal diffusion, the distribution is Gaussian and gives rise to Brownian motion. The curve labeled anomalous has long tails and an infinite second moment, resulting in nonlinear MSD plots and anomalous diffusion. (c) MSD plots for simulations of crowding in an aqueous phase. Simulations done for 75-nm-radius spherical particles in a $3 \times 3 \times 9 \mu\text{m}$ box for 1 ms using the method of Dix et al. (10). (d) (Top) MSD distributions for simulation of 75-nm-radius particles for 10 ms at 9% volume exclusion. The smooth curve is fitted using the expected distribution for normal diffusion. (Bottom) Difference between fitted and observed MSD distributions.

Crowding depresses diffusion (dynamic property)

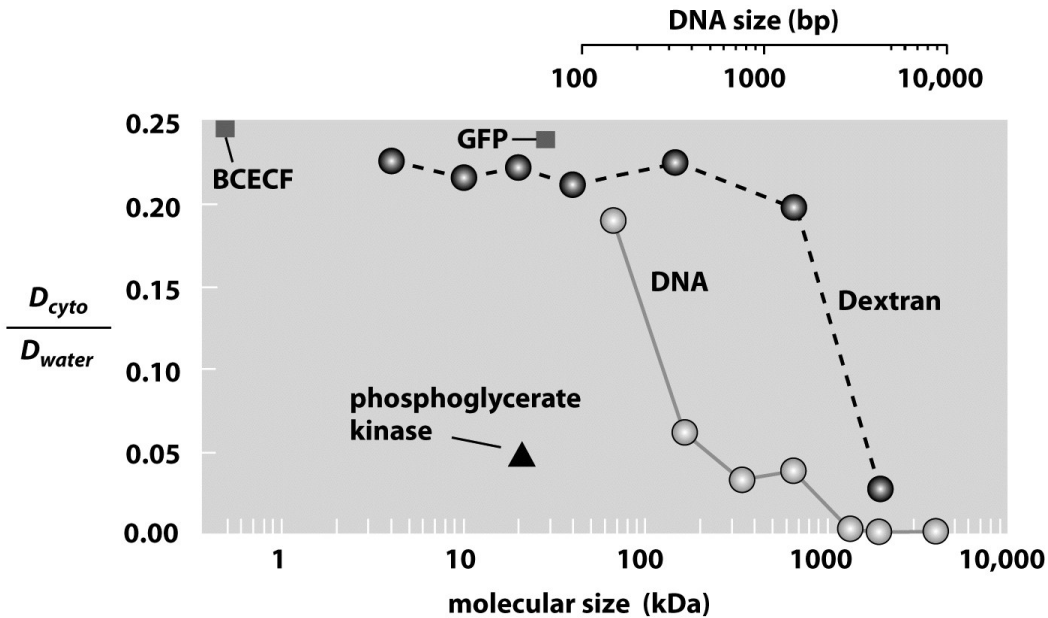


Figure 14.4 Physical Biology of the Cell (© Garland Science 2009)

Figure 14.4 Diffusion constants in cells. The plot shows the ratio of the measured cellular diffusion constant to that for the same molecule in water for several different molecules including a series of DNA molecules of different size. (Adapted from A. S. Verkman, *Trends Biochem. Sci.* 27:27, 2002.)

Substrate channelling

SUMMARY POINTS

1. Crowding can slow the diffusion of solutes in aqueous-phase compartments and in membranes without leading to anomalous diffusion.
2. Large reductions in solute diffusion and/or anomalous diffusion are probably indicators of interactions between the solute and cellular or membrane components, or of fixed barriers to diffusion.
3. Crowding reduces the diffusion of small solutes and many macromolecules in cytoplasm by only a few-fold compared to their diffusion in water.
4. Discrepancies between simulations and experiments on crowding effects on solute diffusion require further investigation.

Counting the states: number of way of arranging indistinguishable objects over boxes...lattice models

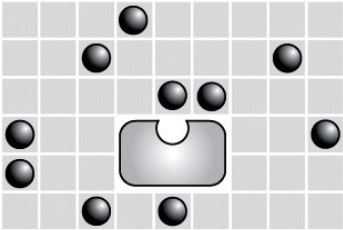
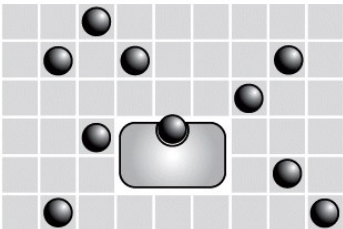
	STATE	ENERGY	MULTIPLICITY	WEIGHT
(A)		$L\epsilon_{sol}$	$\frac{\Omega!}{L!(\Omega-L)!} \approx \frac{\Omega^L}{L!}$	$\frac{\Omega^L}{L!} e^{-\beta L\epsilon_{sol}}$
(B)		$(L-1)\epsilon_{sol} + \epsilon_b$	$\frac{\Omega!}{(L-1)!(\Omega-L+1)!} \approx \frac{\Omega^{L-1}}{(L-1)!}$	$\frac{\Omega^{L-1}}{(L-1)!} e^{-\beta[(L-1)\epsilon_{sol} + \epsilon_b]}$

Figure 6.4 Physical Biology of the Cell (© Garland Science 2009)

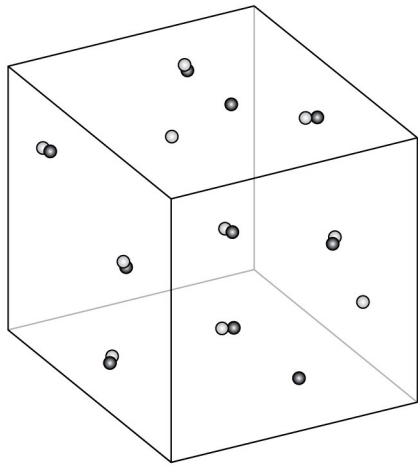
$$p_{bound} = \frac{\sum_{states} \left(\text{grid with hole and 10 spheres} \right)}{\sum_{states} \left(\text{grid with hole and 10 spheres} \right) + \sum_{states} \left(\text{grid with hole and 10 spheres} \right)}$$

Figure 6.5 Physical Biology of the Cell (© Garland Science 2009)

$$p_{bound} = \frac{e^{-\beta \varepsilon_b} \frac{\Omega^{L-1}}{(L-1)!} e^{-\beta(L-1)\varepsilon_{sol}}}{\frac{\Omega^L}{L!} e^{-\beta L \varepsilon_{sol}} + e^{-\beta \varepsilon_b} \frac{\Omega^{L-1}}{(L-1)!} e^{-\beta(L-1)\varepsilon_{sol}}}.$$

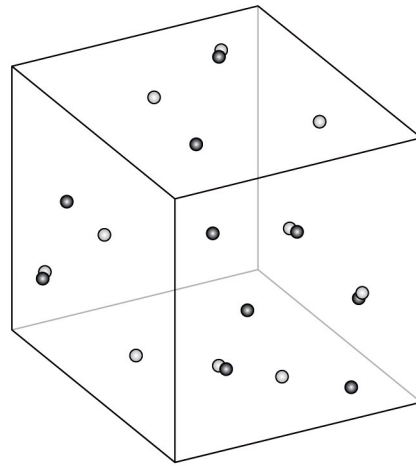
$$p_{bound} = \frac{(L/\Omega)e^{-\beta\Delta\varepsilon}}{1 + (L/\Omega)e^{-\beta\Delta\varepsilon}},$$

$$\Delta\varepsilon = \varepsilon_b - \varepsilon_{sol} \qquad c = L/V_{box} \qquad c_0 = \Omega/V_{box}$$



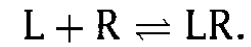
$$K_d = 2.5 \mu\text{M}$$

80% bound



$$K_d = 25 \mu\text{M}$$

50% bound



$$K_d = \frac{[L][R]}{[LR]}.$$

$$p_{\text{bound}} = \frac{[LR]}{[R] + [LR]}.$$

Figure 6

$$p_{\text{bound}} = \frac{[L]/K_d}{1 + ([L]/K_d)}.$$

Langmuir isotherm

$$K_d = \frac{1}{V} e^{\beta \Delta \varepsilon},$$

V is the volume per lattice point

$$p_{bound} = \frac{(c/c_0)e^{-\beta\Delta\epsilon}}{1 + (c/c_0)e^{-\beta\Delta\epsilon}}.$$

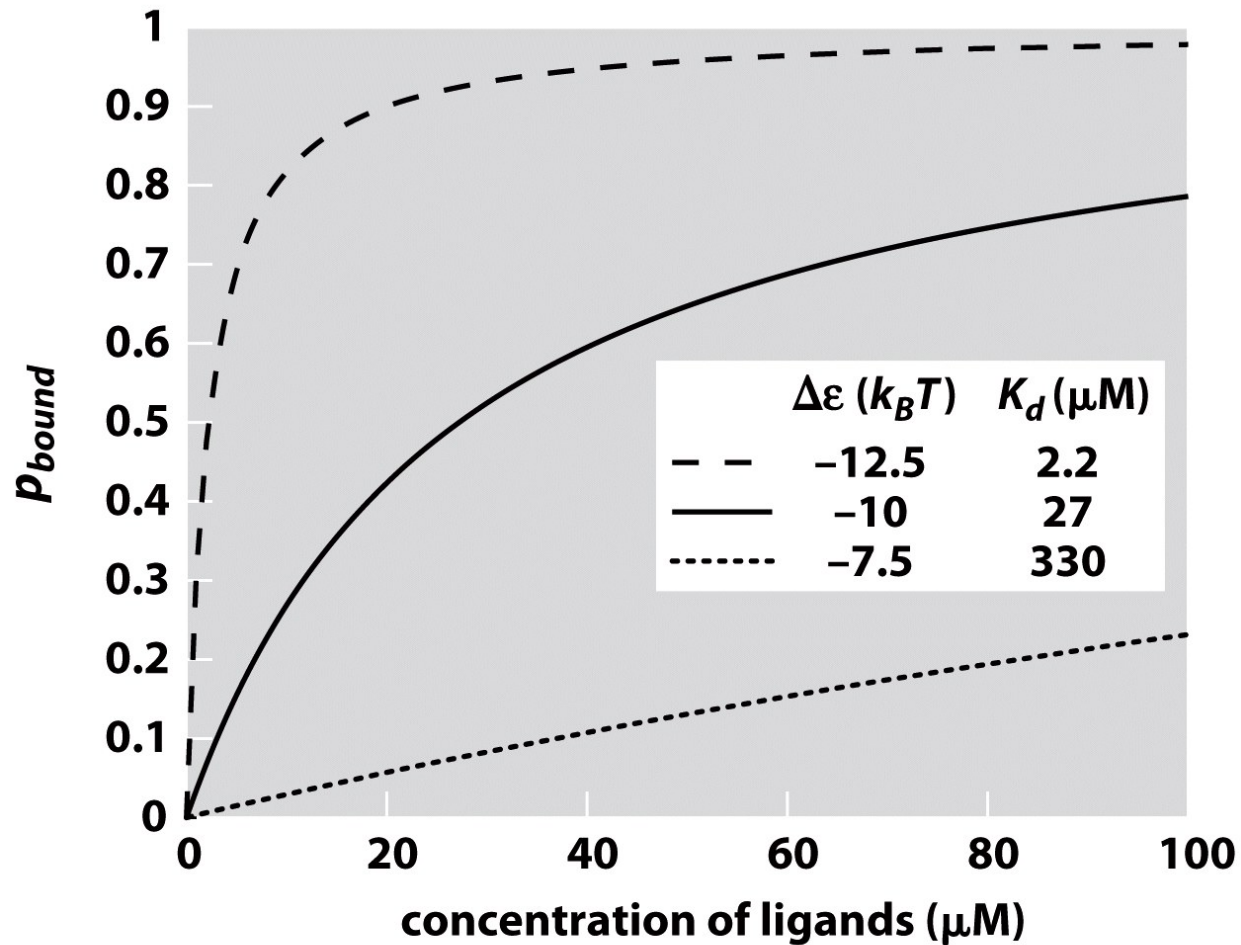


Figure 6.6 Physical Biology of the Cell (© Garland Science 2009)

Crowded variant of the lattice model

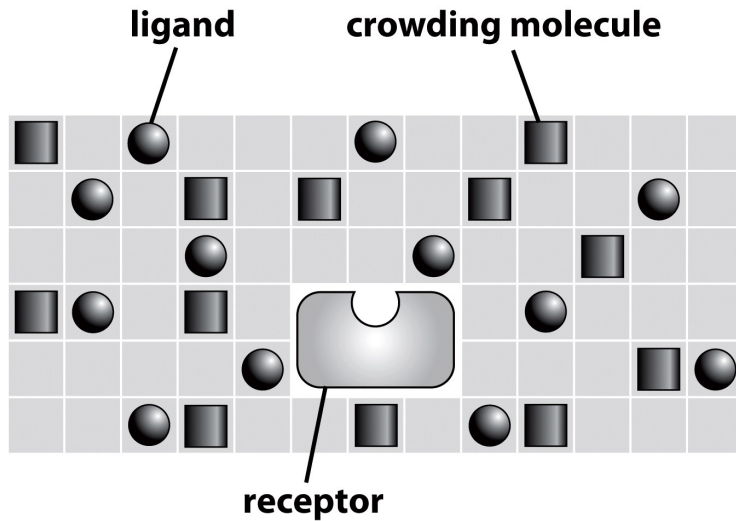


Figure 14.6 Physical Biology of the Cell (© Garland Science 2009)

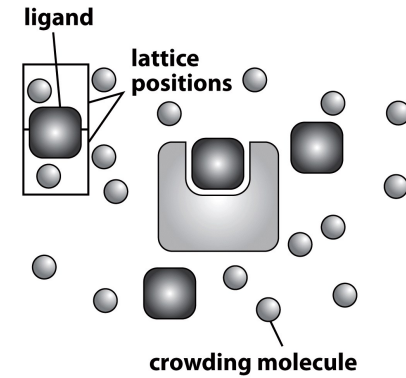


Figure 14.10 Physical Biology of the Cell (© Garland Science 2009)

$$Z_{sol}(L, C) = \frac{\Omega!}{L!C!(\Omega - L - C)!} e^{-\beta L \varepsilon_L^{sol}} e^{-\beta C \varepsilon_C^{sol}},$$

Given this model of the solution, we now ask about the probability that the receptor in solution will be bound by a ligand and how this probability depends upon the concentration of both ligand and crowding molecules. The receptor can be in one of two states: either it has the ligand bound, or not. The weights of these two states are $Z_{sol}(L - 1, C)e^{-\beta \varepsilon_L^b}$ and $Z_{sol}(L, C)$, respectively; ε_L^b is the energy of the ligand bound to the protein. The probability that the ligand will be bound to the protein is therefore,

$$p_{bound} = \frac{Z_{sol}(L - 1, C)e^{-\beta \varepsilon_L^b}}{Z_{sol}(L - 1, C)e^{-\beta \varepsilon_L^b} + Z_{sol}(L, C)}. \quad (14.2)$$

$$p_{bound} = \frac{1}{1 + (\Omega - L - C/L)e^{\beta \Delta \varepsilon_L}},$$

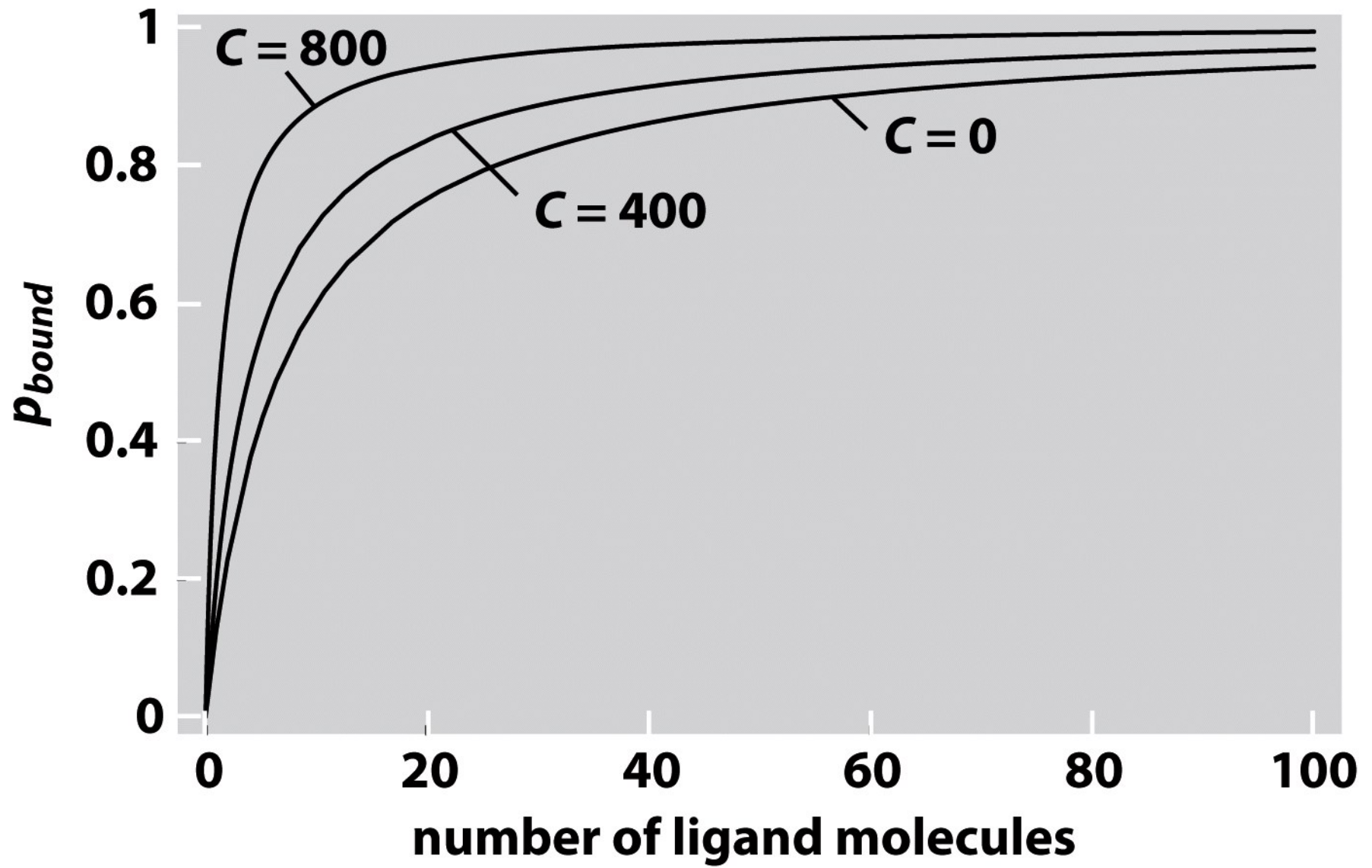


Figure 14.7 Physical Biology of the Cell (© Garland Science 2009)

Crowding enhances ligand binding (static property)

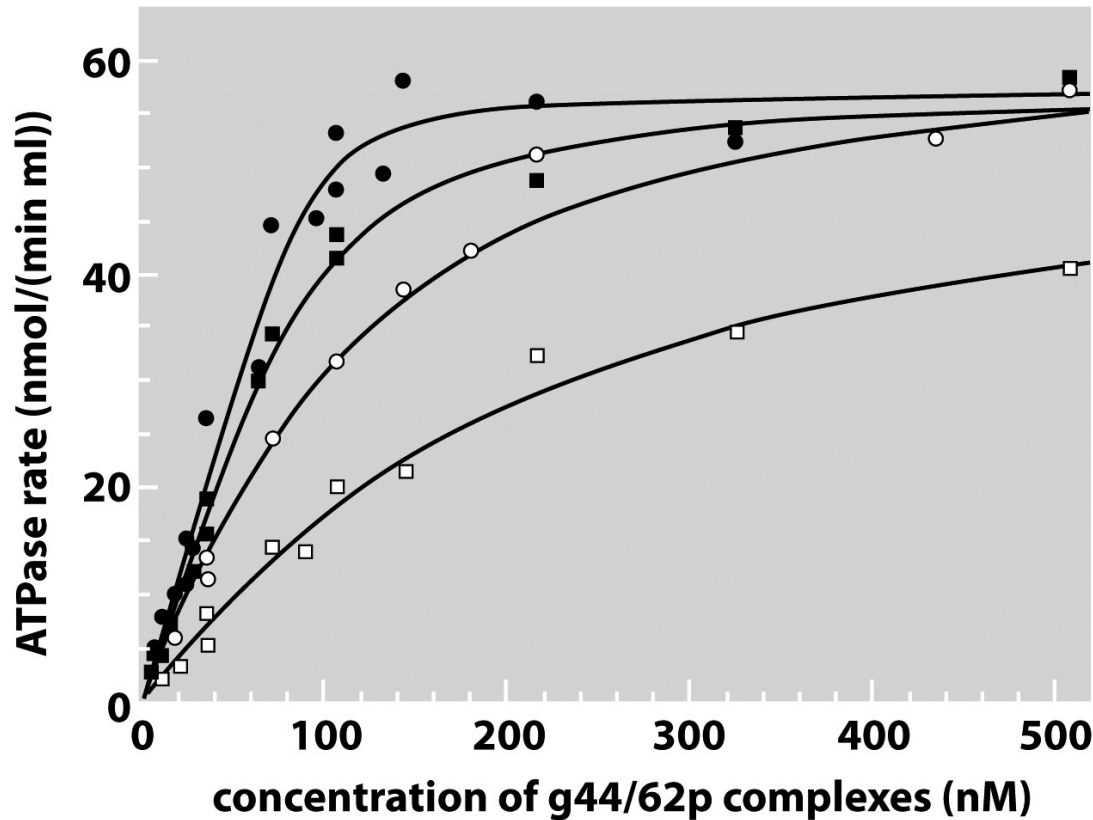


Figure 14.3 Physical Biology of the Cell (© Garland Science 2009)

PEG concentration
from bottom to top:

0, 2.5, 5.0, 7.5 %weight

Figure 14.3 ATPase rate associated with T4 DNA replication. The different curves measure the ATPase rate as a function of the g44/62 protein concentration as measured using different concentrations of polyethylene glycol as a crowding agent. The concentration of polyethylene glycol going from the bottom to the top curve are 0, 2.5, 5 and 7.5 weight percent. (Adapted from T. C. Jarvis et al., *J. Biol. Chem.* 265:15160, 1990.)

Effects of crowding agents on dissociation constants

Renormalized theory

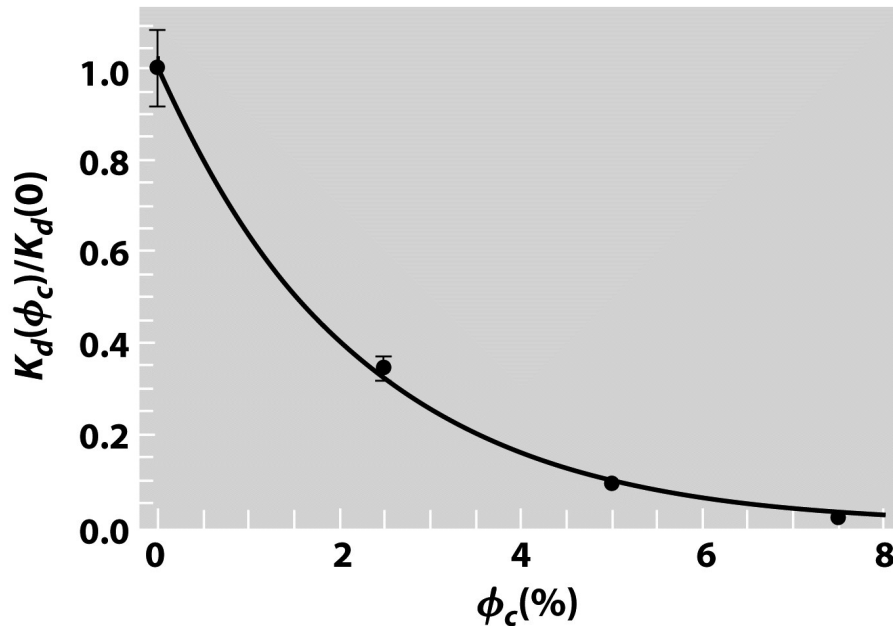


Figure 14.8 Dissociation constant as a function of crowding. Comparison of theory (full line) and experiment (filled circles) for binding in the presence of crowding agents. Measured values of the dissociation constant for gp44/62 and gp45 components of T4 DNA replication complex as a function of polyethylene glycol concentration measured in percent volume fraction. The theoretical curve was obtained by fitting eqn 14.6 for the effective size ratio r of the protein components to the polyethylene glycol 12000 molecules. (Adapted from T. C. Jarvis et al., *J. Biol. Chem.* 265:15160, 1990.)

Figure 14.8 Physical Biology of the Cell (© Garland Science 2009)

$$\frac{K_d(\phi_C)}{K_d(\phi_C = 0)} = (1 - \phi_C)^r.$$

Osmotic pressure in crowded environments: non linear effects

$$Z_{sol}(H, \Omega) = \frac{\Omega!}{H!(\Omega - H)!} e^{-\beta H \varepsilon_H^{sol}}$$

$$G = -k_B T \ln Z_{sol}$$

$$p\nu = G(\Omega - 1) - G(\Omega) = -k_B T \ln \frac{Z_{sol}(H, \Omega - 1)}{Z_{sol}(H, \Omega)},$$

Work = change in free energy

$$p = \frac{k_B T}{\nu} \ln \frac{\Omega}{\Omega - H}, \quad [H] = H / \Omega \nu, \quad p = -\frac{k_B T}{\nu} \ln(1 - [H]\nu).$$

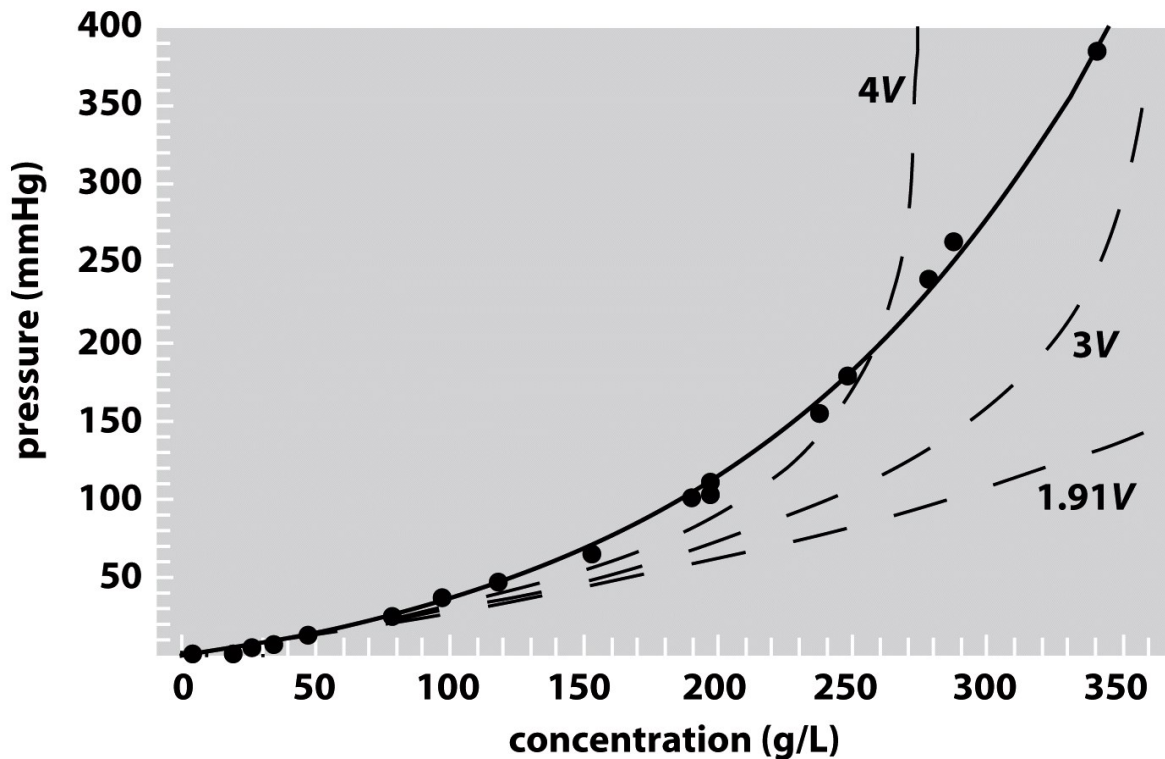


Figure 14.11 Osmotic pressure of a concentrated solution of hemoglobin at 0°C. Filled circles are the experimental data points. The dashed lines are predictions of the lattice gas, while the full line is the pressure of a gas of hard spheres, each sphere having volume V corresponding to a diameter of 5.8 nm. The labels on the curves indicate the volume of a single box in the lattice model. (Adapted from P. D. Ross and A. P. Minton, *J. Mol. Biol.* 112:437, 1977.)

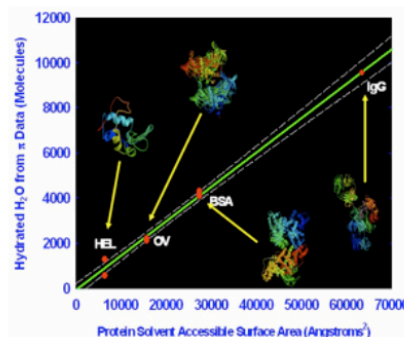
Thermodynamics of Crowded Proteins in Solution

Collaborator: Dr. Ravi Datta

Alumni: Dr. Mohammed Yousef

We are interested in modeling the behavior of concentrated multicomponent protein (crowded) solutions. Crowded protein solutions are found naturally in cells and have tremendous impact on cellular function.

We have modeled the osmotic pressure of both single and binary crowded protein solutions using a novel approach that recognizes that the nonlinear behavior is coupled to hydration and ion binding. This model suggested that the solvent-solute contributions, are substantially more significant in describing osmotic pressure than that assumed by virial expansion models based on McMillan-Mayer theory. When applying the model to single crowded protein solutions in physiological solutions, it was discovered that all of the protein nonideal behavior was coupled to the protein hydration which was directly related to the protein solvent accessible surface area. Interestingly, this significant hydration was always a monolayer of water (see figure). When these factors were taken into account, the solution behaved ideally with respect to the free water (water not interacting with the protein).



Applying the more general form of this model to binary proteins also results in an improved representation of measured osmotic pressure. Our current research investigates the additional contributions of interaction including protein aggregation that can affect osmotic pressure for binary protein systems.

Related Publications

1. Yousef, M. A., Datta, R., and Rodgers, V.G.J., "Monolayer Hydration Governs Nonideality in Osmotic Pressure of Protein Solutions", *AIChE Journal*, 48(6) 1301-1308 (2002).
2. Yousef, M. A., Datta, R., and Rodgers, V.G.J., "Model of Osmotic Pressure for High Concentrated Binary Protein Solutions", *AIChE Journal*, 48(4), 913-917 (2002).
3. Yousef, M. A., Datta, R., and Rodgers, V.G.J., "Confirmation of Free-Solvent Model Assumptions in Predicting the Osmotic Pressure of Concentrated Globular Proteins", *Journal of Colloid and Interface Science* 243 321-325 (2001).
4. Yousef, M. A., Datta, R., and Rodgers, V.G.J., "Understanding Non-Idealities of the Osmotic Pressure of Concentrated Bovine Serum Albumin", *Journal of Colloid and Interface Science*, 207(2), 273-282 (1998).
5. Yousef, M. A., Datta, R., and Rodgers, V.G.J., "Free-Solvent Model of Osmotic Pressure Revisited. Application to Concentrated IgG Solution at Physiological Conditions", *Journal of Colloid and Interface Science*, 197, 108-118 (1998).

Depletion Interactions

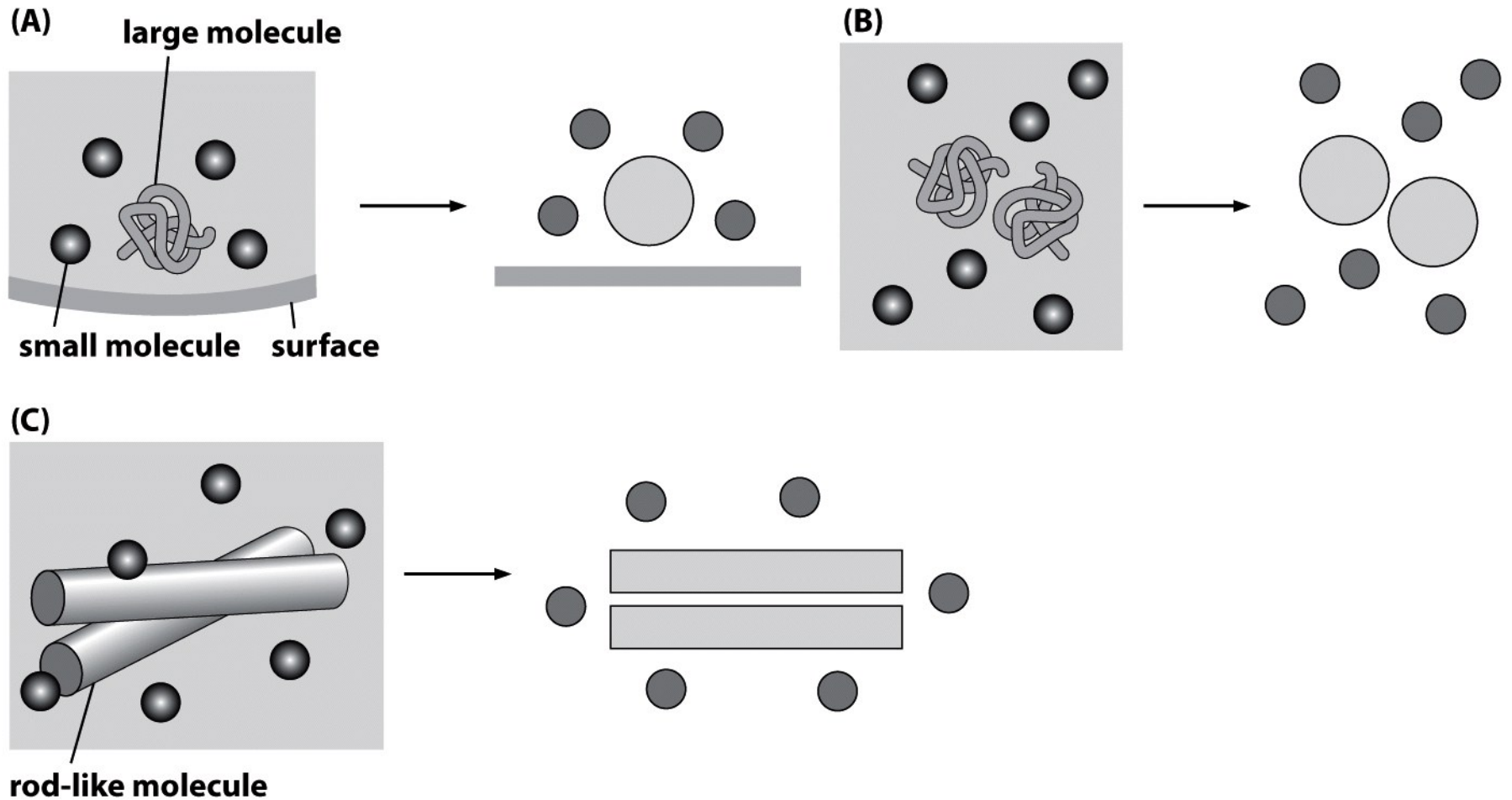


Figure 14.12 Physical Biology of the Cell (© Garland Science 2009)

SEE YOU ON WED. APRIL 19!